Title

DYNAMICS OF THE REACTION OF N+ WITH H9. IV. REACTIVE SCATTERING AT RELATIVE c ENERGIES ABOVE 6 eV

Author

Mahan, Bruce H.

Publication Date

1976-08-01

Submitted to Journal of Chemical Physics

LBL-5454
Preprint c.1

DYNAMICS OF THE REACTION OF N^+ WITH H_2. IV. REACTIVE SCATTERING AT RELATIVE ENERGIES ABOVE 6 eV

Bruce H. Mahan and W. E. W. Ruska

August 18, 1976

Prepared for the U. S. Energy Research and
Development Administration under Contract W-7405-ENG-48

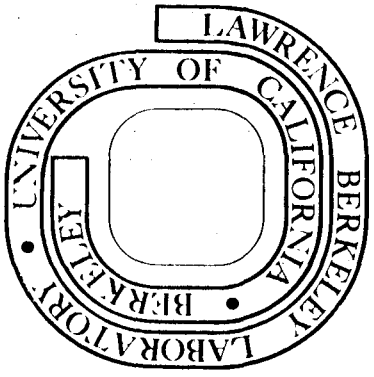

DISCLAIMER

DYNAMICS OF THE REACTION OF N^+ WITH H_2. IV. REACTIVE SCATTERING AT RELATIVE ENERGIES ABOVE 6 eV

Bruce H. Mahan and W. E. W. Ruska

Department of Chemistry and Materials and Molecular Research Division of the Lawrence Berkeley Laboratory, University of California, Berkeley 94720

ABSTRACT

Product velocity vector distributions for the reaction $N^+(H_2,H)NH^+$ and its isotopic variants have been determined in the range of relative energies above 6 eV. The reaction is direct, and there is a critical relative energy above which the spectator stripping peak disappears and is replaced by a double intensity lobe structure. Some evidence of the reaction of electronically excited metastable ions, probably $N^+(^1D)$, is found. The results are compared with the predictions of the sequential impulse model of reactive scattering. The agreement is generally good, except that more very large angle scattering is observed, particularly for the $N^+(HD,H)ND^+$ case, than is predicted by the model.

Product velocity vector distributions have been measured for a substantial number of ion-molecule reactions.[1] One of the features most characteristic of direct exoergic hydrogen atom transfer reactions of the type $A^+(H_2,H)AH^+$ in the low to intermediate relative energy range is the appearance in the product velocity distribution of a very prominent peak at the spectator stripping velocity. The internal energy of the product formed by spectator stripping increases linearly with increasing initial relative energy. It was predicted[2] that at the critical initial relative energy at which the internal energy of the stripped product first exceeds its dissociation energy, the stripping feature would be lost.

Experiments have shown this to be true only in a restricted sense. For the reactions[3-5] of N_2^+, CO^+, and Ar^+ with H_2, the intense forward peak in the distribution does not disappear above the critical energy, but instead moves forward from the spectator location to higher relative speed where the product is stable. Thus a relatively intense peak in the forward recoil direction persists for initial relative energies well above the critical spectator limit. Only in one reaction,[6,7] $O^+(H_2,H)OH^+$, is the spectator stripping peak entirely lost when the relative energy exceeds the spectator limit.

Since the reactions of N_2^+, CO^+, and Ar^+ with H_2 are markedly exoergic ($\Delta H \simeq -1.4$ eV) and the $O^+(H_2,H)OH^+$ reaction is less so ($\Delta H = -0.4$ eV), it seems reasonable to connect exoergicity with the feature of the potential energy surface

which makes direct forward recoil possible. Inasmuch as the reaction $N^+(H_2,H)NH^+$ is very nearly thermoneutral and shows a spectator stripping peak in the intermediate relative energy (2-7 eV) range, it appeared that it would be of value to investigate the reactive scattering in this system at high initial relative energies. In what follows, we report product velocity distributions for the reactions of N^+ with H_2 and HD, and compare these results with the predictions of the sequential impulse model[7,8] (SIM) of direct chemical reactions.

Experimental

The apparatus used in this work has been described in detail previously.[9] The experiments are performed by allowing a collimated, energy selected beam of N^+ ions to impinge on a target gas contained in a scattering cell. The scattered ions pass through an electrostatic energy analyzer and a quadrupole mass filter before being detected by an ion counter. The detector components and exit aperture of the scattering cell are mounted on a rotatable lid, which permits the intensity of scattered ions to be measured at various angles and energies.

In most experiments, N^+ ions were extracted from a microwave discharge through a 9:1 N_2-He mixture. In previous studies,[7,10] this type of discharge has been shown to produce ions predominantly in their electronic ground states. To ascertain the state composition of the N^+ beam more directly, attenuation experiments of the type described by Rutherford and Vroom[11] were carried out. These showed that the fraction

of metastable excited N^+ from N_2-He discharges was no more than 0.03. Other experiments were performed with N^+ drawn from microwave discharges through mixtures of ammonia or nitrous oxide with argon. In the former case, a metastable excited state population of approximately 3% was found, while in the latter case, 6% of the beam consisted of metastable excited ions.

Our experimental results are presented in the form of contour maps of the specific intensity $\bar{I}(\theta,u)$, the intensity of ions per unit velocity space volume normalized to unit beam strength, scattering gas density, and collision volume. A polar coordinate system is used, with the radial coordinate u representing the speed of the ion relative to the center of mass velocity of the complete target-projectile system, and the angular coordinate θ measured with respect to the original direction of the projectile ion beam. The specific intensity is normalized such that

$$\bar{\sigma} = 2\pi \int_0^{\pi} \sin\theta d\theta \int_0^{\infty} u^2 \, \bar{I}(\theta,u) \, du$$

is always proportional to the true total cross section σ.

Results

Figure 1 shows a contour map of the specific intensity of NH^+ from the reaction of N^+ with H_2 at an initial relative energy of 6.87 eV. The product distribution is very similar to those found in investigations of several hydrogen atom abstraction reactions in the low to intermediate energy range,

and is in agreement with the results of an earlier investigation.[12] The asymmetry of the distribution about the ±90° axis indicates that the reaction proceeds by a direct interaction mechanism. The intensity maximum occurs at the spectator stripping velocity. Compared with the distributions from other direct ion-molecule reactions, the stripping peak in Fig. 1 is somewhat broader and less prominent relative to the large angle scattering.

Figure 2 shows the product velocity distribution from the $N^+(H_2,H)NH^+$ reaction run at an initial relative energy of 12.5 eV. At this energy the spectator stripping velocity lies within the circular zone of product instability defined by the translational exoergicity Q assuming the value -4.6 eV. For values of the final relative speeds which correspond to $Q \leq -4.6$ eV, the $^2\Pi$ ground state of NH^+ is unstable with respect to dissociation to N^+ and H. The $^4\Sigma^-$ state of NH^+, which is nearly degenerate with the $^2\Pi$ ground state at the equilibrium separation, dissociates[13] to $N(^4S)$ and H^+, and is unstable for Q values less than -3.7 eV. It is clear that the peak at a scattering angle of zero degrees which was so prominent at lower energies has disappeared at this higher energy, and has been replaced by two intensity maxima at ±60°. This is just the general behavior predicted[7,8] by the Sequential Impulse Model (SIM) for a thermoneutral abstraction reaction. Similar behavior was observed in the investigation of the $O^+(H_2,H)OH^+$ reaction.

It will be noticed in Fig. 2 that the product intensity at zero degrees is small, but not equal to zero, as might be expected from the SIM or from the primitive stripping model. This might be a consequence of the finite primary ion beam width, or of the difficulty of removing the contribution of the reaction of N^+ with the background gas in the detector train. On the other hand, the possibility that this small forward scattered component might represent a contribution from a legitimate dynamical process led us to examine the reaction at still higher energy. These experiments were difficult because the cross section for the production of NH^+ is very small at these high relative energies.

Figure 3 shows the NH^+ distribution obtained from N^+-H_2 collisions at 15.6 eV initial relative energy. It was ascertained that the large angle scattering at this energy was of very small intensity, and it was not investigated in detail. The double lobe structure at $\pm 60°$ expected from the SIM is evident in Fig. 3. In addition, there is a component in the very small angle region which is of comparable importance. This small angle component lies forward of the spectator stripping point, in the velocity zone in which the product is stable. Thus, part of the reactive scattering does display the direct forward recoil which is expected only from exoergic reactions.

Since the SIM indicates that forward recoil of the product at exactly zero degrees must come from reaction exoergicity, the NH^+ in the small angle high velocity region may come from

the reaction with H_2 of N^+ which is in a metastable excited electronic state. To ascertain whether or not this is true, we investigated the high energy reactive scattering of N^+ drawn from microwave discharges through NH_3 - Ar and N_2O - Ar mixtures, and compared the results with the concentration of metastable N^+ as determined by the beam attenuation method.[11]

Figure 4 shows the NH^+ distribution obtained at 15.6 eV initial relative energy using N^+ prepared by a microwave discharge through an N_2O - Ar mixture. Relative to the two large angle lobes, the small angle peak is clearly more prominent than it is in Fig. 3. The attenuation method showed that the beam from the N_2O - Ar mixture contained approximately 6% metastable excited N^+. A similar experiment was run using a microwave discharge through an NH_3 - Ar mixture to prepare N^+. The relative prominence of the small angle scattering was intermediate between the results displayed in Figs. 3 and 4, and the beam attenuation results showed that the concentration of metastable excited N^+ had an intermediate value, approximately 3%. The correlation of the very small angle product intensity component with the fraction of metastable N^+ in the beam makes it highly likely that the part of the reaction which displays forward recoil comes from the reaction of N^+ in one of its lower metastable stables (^1D,^1S,^5S) to give NH^+ in its ground electronic state. A recent investigation in our laboratory[14] of the $N^+(H_2,H)NH^+$ reaction at very low initial relative energies has also produced clear evidence of forward recoiled NH^+ formed by

reaction of $N^+(^1D)$ with H_2. It is of interest to note that the velocity vector distributions show evidence of the metastable excited reactant only at very high or very low initial relative energies.

In order to provide more experiments which would test the SIM, we investigated the reaction of N^+ with HD, and measured both the NH^+ and ND^+ velocity vector distributions. Figure 5 shows the NH^+ from N^+-HD collisions at an initial relative energy of 9.7 eV. At this energy, the spectator stripping peak lies just within the zone of stable product velocities. The observed vector distribution is strongly peaked in the forward direction, and the intensities in the small angle region are significantly greater, relative to the large angle scattering, than in the case of the $N^+(H_2,H)NH^+$ reaction.

One of the distributions of NH^+ from N^+-HD collisions at higher initial reactive energy is shown in Fig. 6. The spectator stripping point lies in the unstable product zone, and the double lobe structure observed in other high energy experiments is present. Note that the lobes occur at smaller scattering angles that was the case for the $N^+(H_2,H)NH^+$ reaction at a similar relative energy (Fig. 2).

At an initial relative energy of 6.55 eV, ND^+ formed by spectator stripping from N^+-HD collisions just becomes unstable. A velocity vector distribution for the $N^+(HD,H)ND^+$ reaction was determined at this relative energy, and showed the expected double lobe structure with no peak at the spectator

stripping velocity. There was also prominent ND^+ intensity at large scattering angles. In fact, we observed a nearly constant angular distribution from 60° to 180°, which was approximately two-thirds as intense as the lobes in the forward scattering region. This propensity for the deuterated product to be scattered at larger angles than the protonated product in ion reactions with HD has been observed previously, most notably[6,7] in the O^+-HD reaction.

The distribution of ND^+ formed from collisions of N^+ with HD at an initial relative energy of 9.7 eV is shown in Fig. 7. The double lobe structure has disappeared, virtually all the product appears in the backward scattering region, and there is an intensity peak at 180°. An experiment was also carried out at an initial relative energy of 12.3 eV, and the ND^+ was found to have a distribution similar to that of Fig. 7, with the peak at 180° relatively more prominent, if lower in absolute intensity.

A number of experiments were performed in which the distribution of N^+ scattered non-reactively by H_2 or D_2 was measured. The results of the experiments done at the lowest and highest relative energies are shown in Figs. 8 and 9 respectively. Even at initial relative energies as low as 6.87 eV, there is very little detectable large angle non-reactive scattering. As Fig. 8 shows clearly, the large angle scattering and some of the small angle scattering is quite inelastic. As the relative energy is increased, the small amount of non-reactive scattering which is observed is

confined to smaller and smaller angles. Therefore, in this high energy regime, collisions between N^+ and H_2 which are head-on, or nearly so, essentially always lead to the disappearance of N^+ either by reaction to form NH^+, or by charge transfer to give H_2^+ or H^+.

It is of interest to note that in Fig. 9, all the non-reactive scattering is confined to small angles. There is no evidence of any N^+ scattered impulsively from one of the target atoms. Such impulsive features were found[7,15] to be prominent in the non-reactive scattering of O^+ by H_2, HD, and D_2, and they were considered to be one of the clearest indications that the SIM might describe the reactive scattering well. The absence of impulsive non-reactive scattering in the N^+-H_2 system does not necessarily mean that the impulsive model for reactive scattering is inappropriate. The total intensity of N^+ scattered non-reactively is small, and the component which might be scattered impulsively from one target atom could very easily be below the sensitivity of the detection system.

The observations that both the non-reactive and the reactive scattering are of low total intensity suggest that charge transfer to form H_2^+ or H^+ are the dominant product channels at high relative energy. We are unable to make measurements of the angular distributions of H_2^+ and H^+, or even to identify the masses of the ions formed by charge transfer. However, we are able to collect the ions formed in the scattering cell with velocities which are much smaller

than that of the projectile ions. When N^+ is incident on H_2 with a relative energy of 8.7 eV, the slow ion current amounts to approximately 60% of the beam attenuation. Since the collected slow ion current is a lower limit for the amount of charge transfer, the results indicate that charge transfer is the dominant collision process in the range of relative energies investigated in this work.

Discussion

Many of the features of the product distributions can be interpreted with the aid of the partial state correlation diagram[16] which is reproduced in Fig. 10. When $N^+(^3P)$ approaches H_2 collinearly, it may move on a doubly degenerate $^3\Pi$ surface which leads adiabatically to $NH^+(^2\Pi)$ and $H(^2S)$, the ground state products. No deep wells or barriers are expected along this path. Upon bending, this $^3\Pi$ surface splits into $^3A'$ and $^3A''$ surfaces, which become $^3A_1$ and $^3A_2$ as the isosceles triangle conformation is reached. The former (not shown on the diagram) involves an excited configuration, but the latter is the lowest $^3A_2$ state formed when $N^+(^3P)$ approaches H_2 along the bisector of the bond axis. Merely by using symmetry arguments supplemented by qualitative considerations based on molecular orbital configurations it is not possible to characterize this $^3\Pi$ - $^3A''$ - $^3A_2$ surface quantitatively. However, the nature of the $^3A_2$ surface has been elucidated by an SCF-CI calculation performed by Schaefer et al.[17] This calculation reveals a relatively shallow (~2.5 eV) potential energy well at large N^+-H_2 distances when the H_2 distance is

slightly expanded. Thus at large N^+-H_2 distances, the $^3A_2$ surface does lie low in energy, and from this we conclude that the complete $^3\Pi$ - $^3A''$ - $^3A_2$ potential surface of N^+-H_2 provides a relatively flat, angle independent path between reactants and products. It is this type of surface which should lead to product distributions similar to those predicted by the SIM, which incorporates an angle independent potential.

Figure 10 also shows that collinear approach of $N^+(^3P)$ towards H_2 can put the system on a $^3\Sigma^-$ surface which leads to $NH^+(^4\Sigma^-)$ and $H(^2S)$. Consideration of the molecular orbital configuration suggests that this surface may have a shallow well along the reaction path, and may also have a low energy barrier in the product channel. If this were true, approximately one-third of the very low energy N^+-H_2 collisions would be non-reactive, and this would help to account for the fact that the thermal (300K) rate constant for the $N^+(H_2,H)NH^+$ reaction is approximately one-half the ion-induced dipole capture rate constant.[18] Upon bending, the $^3\Sigma^-$ surface becomes $^3A''$ and eventually $^3B_1$ in the isosceles triangle geometry. At large N^+-H_2 distances, this $^3B_1$ state is the highest of the three states formed as $N^+(^3P)$ approaches H_2 along the perpendicular bisector of the bond. Thus the $^3\Sigma^-$ - $^3A''$ - $^3B_1$ surface would appear to be angle dependent, and at least initially should tend to favor a collinear approach of N^+ toward H_2. It is also of interest to note that non-adiabatic behavior on this surface is possible, and can lead to the charge

transfer products $NH(^3\Sigma^-)$ and H^+, or N and H_2^+. Without a detailed knowledge of the nature of the avoided crossings which can lead to charge transfer it is impossible to predict how important it should be. However, the likely existence of such avoided crossings does allow a rationalization of the importance of charge transfer which was observed experimentally.

The correlation diagram provides a rationalization of the forward recoiled NH^+ which is observed at high relative energies, and is associated with metastable excited N^+. One component of the states which arise when $N^+(^1D)$ approaches H_2 collinearly is a $^1\Pi$ surface. This surface correlates with $NH^+(^2\Pi)$, and the full exoergicity of approximately 2 eV is in principal available to help provide product stabilization by forward recoil, as evidently occurs in the exoergic reactionsof N_2^+, CO^+, and Ar^+ with H_2.

Since the $^3\Pi$ - $^3A''$ - $^3A_2$ surface is expected to have characteristics which are approximately those assumed in the SIM of high energy reactions, it is worthwhile to compare the observed product distributions with the predictions of this simple model. A detailed account of the SIM has been given elsewhere,[8] and here we will only briefly summarize its principal features.

The SIM predicts that for the reaction A(BC,C)AB, the product distribution may consist of two distinct components: a spectator stripping feature which involves collisions in which A hits B, AB is formed, and C is undisturbed, and a

"hard sphere" feature which results from A hiting B elastically and impulsively, B hiting C in a like manner, and AB being formed if its internal energy is less than its dissociation energy. The internal energy and final translational energy of the products are completely determined by the sequence of two separate elastic impulses.

The general shape of the product distribution is largely determined by two factors. One is a limiting cardioid in velocity space which gives at any angle the maximum product translational energy which can be achieved by a sequence of two elastic impulses. The spectator stripping event occurs at the cusp of the cardioid. The low speed limit for products is provided by the stability circle, which is the smallest final translational speed that the products can have and be stable with respect to dissociation.

Examples of the limiting cardioids and stability circles appear in the SIM distributions of Fig. 11. The size of the limiting cardioid depends[8] on the initial relative velocity V_1 and the masses only through the quantity

$$R = V_1 \left(\frac{A}{A+B}\right)\left(\frac{B}{B+C}\right)$$

where the letters represent the masses of the atoms. Thus the cardioid scales with V_1, and only one cardioid is needed to represent the limiting product velocity for all initial velocities and all isotopic variations, provided the scale of the drawing is changed appropriately. To facilitate comparison between the various isotopic cases, all the cardioids in Fig. 11

have been taken to be of the same size, and accordingly, location of the center of mass velocity within the cardioid, and the length of the projectile velocity vector change as isotopic substitutions are made.

The stability circles always have the center of mass as their origin, and they do not scale with the initial relative velocity. Therefore, stability circles for different initial relative energies must be drawn for each isotopic case. As Fig. 11 shows, the stability zone of velocities for the AB product is largest at low initial relative velocities, and decreases toward zero as infinite initial relative velocity is approached. A particularly significant initial relative velocity is the one at which the stability circle first intersects the cardioid at the cusp. At this energy, the spectator stripping peak should disappear. Above this energy, the distribution should have the double lobe structure which is evident in the experimental results of Figs. 2 and 6.

The intensity and, to a much lesser degree, the detailed shape of the hard sphere component of the distribution are controlled by the factor d_{23}/r_o, the ratio of the mutual hard sphere diameter of B and C to their bond distance in the BC molecule. In the special case where this ratio is equal to unity, the intensity contours are circles concentric with the cusp of the limiting cardioid, and the intensity falls off as the inverse square of their radii. This is the case plotted in Fig. 11. For smaller values of d_{23}/r_o, the hard sphere distribution rises more rapidly in the small angle

region, but is relatively unchanged at large angles. Of course, as d_{23}/r_o decreases, the total intensity of the two-impulse hard sphere component decreases, and the fraction of spectator type collisions increases.

The foregoing discussion and Fig. 11 indicate that in the various isotopic experiments, the product distribution which might be detected is fundamentally the same except for the location of the stability circles relative to the limiting cardioid and the location of the center of mass relative to the stable product velocity zone. Thus, according to the primitive SIM, isotope effects in angular distributions have a relatively simple origin.

In comparing the predictions of the SIM with experiment, we must be aware that the calculated distributions have not been averaged over the projectile velocity spread and the detector bandpass. Such averaging would be possible, of course, for any case desired, but it would then not be feasible to represent the predictions of the SIM in the compact form of Fig. 11. To begin with the N^+-H_2 system at 6.9 eV, we note that the predictions of Fig. 11 are in general accord with this experimental results of Fig. 1. That is, the spectator stripping peak is predicted to be in a stable region as is observed experimentally, and the predicted intense scattering out to about 45° is observed. The very large angle scattering appears to be relatively a bit more intense experimentally than is predicted by the SIM.

Much the same can be said for the $N^+(HD,D)NH^+$ reaction at 9.7 eV. The spectator stripping and intense forward scattering predicted in Fig. 11 is in fact observed in Fig. 5. However, Fig. 11 indicates that there should be no NH^+ product from N^+-HD collisions at angles greater than 85°, and such large angle scattering is apparent, although of quite weak intensity in Fig. 5. The ND^+ distribution from N^+-HD collisions at 6.5 eV, which we do not show, is also generally consistent with the predictions of the lowest panel of Fig. 11. That is, the spectator stripping peak is absent, two intensity maxima occur in the small angle (~30°) scattering region, and product is observed at all larger scattering angles. The most obvious discrepancy is that the scattering in the very large angle region is somewhat more intense relative to the small angle scattering than is predicted by the SIM.

If we consider higher relative energies, we see that for the N^+-H_2 system at 12.5 eV, Fig. 11 predicts no spectator stripping, a double lobe pattern of intensity at small angles, and very weak backscattering with no intensity in the region around 180°. The lobe structure is found in Fig. 2, as predicted. It must be stressed that the position and general appearance of the lobes are highly influenced by the angular resolution of the detector. This may explain the appearance of the lobes at ±60° in Fig. 2, rather than at a smaller pair of angles which might be expected from Fig. 11. The large angle scattering in Fig. 2 is weak, but again is probably more intense than is expected from the SIM.

For the $N^+(HD,D)NH^+$ reaction at 12.5 eV, Fig. 11 predicts a pair of intensity maxima at small angles, and no spectator stripping or backscattered product. This is consistent with the experiment of Fig. 6. Note also that the NH^+ lobes from HD appear at smaller angles than those from H_2, as Fig. 11 suggests.

The most serious discrepancy between experiment and the SIM occurs for the $N^+(HD,H)ND^+$ reaction at 9.7 eV and above. Figure 11 suggests that a crescent shaped distribution with intensity maxima in the small angle region and an intensity minimum at 180° should be observed. Figure 7 in fact shows very little forward scattering, and an intensity maximum at 180°. Thus, apart from the fact that the SIM predicts that backscattering should be more important in this isotopic system than in any other, the model and the experiment are here in clear disagreement.

Given our lack of knowledge about the detailed potential energy surfaces, it is unlikely that any completely satisfactory explanation for the partial failure of the SIM can be advanced with certainty. However, certain possibilities are evident. The discrepancy is that in all isotopic cases, and particularly in the $N^+(HD,H)ND^+$ system, there is more product intensity at 180° than is predicted by the SIM. Scattering at 180° comes from collinear or near collinear collisions. For the collinear NHH^+ and NHD^+, the kinematic angle[6,19] β between the asymptotic reactant and product troughs of the skewed potential surface is 48.8° and 31.3° respectively. This means that collinear

events in these systems should lead to multiple impulse or chattering collisions[7] which are not in the SIM. While it is difficult to predict what the results of such chattering collisions will be, the possibility of their occurrence makes the observed deviations from SIM behavior in the large angle region much less surprising.

For the collinear NDH^+ system, the kinematic angle β is 67.6°. This will not produce multiple collision phenomena. In fact, ND^+ with relative low internal excitation is produced by a binary impulse sequence which is completely incorporated in the SIM. It is this favorable outcome of the binary collision sequence for collinear and near collinear collisions which is responsible for the large angle ND^+ intensity predicted by the SIM. What is not predicted is the peak at 180°.

So far our discussion has been concerned with only the $^3\Pi$ - $^3A''$ - $^3A_2$ surface which leads to ground state products and has the flat, angle independent features which are consistent with the SIM. We have noted, however, that the $^3\Sigma^-$ - $^3A''$ - $^3B_1$ surface has features which might encourage a collinear approach. This surface also forms NH^+ in its $^4\Sigma^-$ state, which, since it dissociates to $N(^4S)$ and H^+, is approximately 1 eV less stable than the $^2\Pi$ ground state of NH^+. The following argument then presents itself. There may be an important tendency for scattering on the $^3\Sigma^-$ - $^3B_1$ surface to follow near collinear paths. Most of the other types of collisions on this surface may lead to charge transfer, or to transient product which is unstable with respect to dissociation. The $NH^+(^4\Sigma^-)$ product

which is most likely to be stable is that formed by collinear or near collinear collisions on this surface. This is most obvious for the NDH^+ mass combination because this is the only combination which can, according to the impulse model, produce stable backscattered ND^+ or NH^+ in either the $^2\Pi$ or $^4\Sigma^-$ states at high energy. In this manner we can rationalize the ND^+ intensity peak at 180°. A decision as to whether or not this is the correct rationalization will have to await detailed information on the nature of the lower potential surfaces in this system.

Summary

We have shown that the thermoneutral reaction of ground state N^+ with H_2 to give ground state NH^+ and its isotopic variants in large degree follow the type of dynamics predicted by the sequential impulse model. That is, there is a critical energy at which the spectator stripping peak disappears and is replaced by a double lobe structure, and in the reaction with HD, the protonated product is scattered preferentially to much smaller angles than the deuterated product. More large angle scattering is observed experimentally than is expected from the SIM, particularly in the case of ND^+ from HD. This is rationalized as due to contributions from an angle dependent potential surface which favors collinear collisions, and which is most likely to produce stable product when the isotopic arrangement is NDH^+. We have also detected the direct forward recoil of NH^+ formed by the exoergic reaction of $N^+(^1D)$ with H_2.

Acknowledgement

This work was done with support from the U. S. Energy Research and Development Administration.

References

1. For reviews of the recent literature, see W. S. Koski, in "Advances in Chemical Physics," vol. 30, edited by K. P. Lawley (Wiley-Interscience, New York 1975) and B. H. Mahan in International Review of Science, Physical Chemistry Series II, vol. 9, edited by D. R. Herschbach (Butterworths, London, 1976).
2. A. Henglein, Advan. Chem. Ser. 58, 63 (1966).
3. K. Lacmann and A. Henglein, Ber. Bunsenges. Phys. Chem. 69, 292 (1965).
4. M. Chiang, E. A. Gislason, B. H. Mahan, C. W. Tsao, and A. S. Werner, J. Chem. Phys. 52, 2698 (1970).
5. L. Doverspike, R. Champion, and T. Bailey, J. Chem. Phys. 45, 4385 (1966).
6. K. T. Gillen, B. H. Mahan and J. S. Winn, J. Chem. Phys. 58, 5373 (1973).
7. K. T. Gillen, B. H. Mahan and J. S. Winn, J. Chem. Phys. 59, 6380 (1973).
8. B. H. Mahan, W. E. W. Ruska and J. S. Winn, J. Chem. Phys. (to be published).
9. W. R. Gentry, E. A. Gislason, B. H. Mahan and C. W. Tsao, J. Chem. Phys. 49, 3058 (1968).
10. M. H. Chiang, E. A. Gislason, B. H. Mahan, C. W. Tsao and A. S. Werner, J. Phys. Chem. 75, 1426 (1971).
11. J. A. Rutherford and D. A. Vroom, J. Chem. Phys. 62, 1460 (1975).
12. E. A. Gislason, B. H. Mahan, C. W. Tsao and A. S. Werner, J. Chem. Phys. 54, 3897 (1971).

13. H. P. D. Liu and G. Verhaegen, J. Chem. Phys. 53, 735 (1970).

14. J. M. Farrar, S. G. Hansen and B. H. Mahan, J. Chem. Phys. (to be published).

15. K. T. Gillen, B. H. Mahan and J. S. Winn, Chem. Phys. Letters, 22, 344 (1973).

16. J. A. Fair and B. H. Mahan, J. Chem. Phys. 62, 515 (1975).

17. C. F. Bender, J. H. Meadows and H. F. Schaefer III (to be published).

18. F. C. Fehsenfeld, A. L. Schmeltekopf and E. E. Ferguson, J. Chem. Phys. 46, 2802 (1967).

19. B. H. Mahan, J. Chem. Ed. 51, 308, 377 (1974).

Figure Captions

Fig. 1. A contour map of the specific intensity of NH^+ from the $N^+(H_2,H)NH^+$ reaction at an initial relative energy of 6.87 eV. The small cross marks the spectator stripping velocity, and the small circles locate the intensity maxima along the ridge of the crater-like intensity distribution.

Fig. 2. A contour map of the specific intensity of NH^+ from N^+-H_2 collisions at an initial relative energy of 12.5 eV. Note the double lobe structure and the absence of a peak at $\theta=0°$.

Fig. 3. The specific intensity of NH^+ from N^+-H_2 collisions at 15.6 eV initial relative energy. Note the very low overall intensity and the broad peak at 0° as well as the lobe structure at ±60°.

Fig. 4. The specific intensity of NH^+ from N^+-H_2 collisions at 15.6 eV initial relative energy. The N^+ was drawn from a microwave discharge through an N_2O-Ar mixture, and contained approximately 6% metastable excited N^+.

Fig. 5. The intensity distribution of NH^+ from N^+-HD collisions at 9.7 eV initial relative energy.

Fig. 6. The intensity distribution of NH^+ from N^+-HD collisions at 12.3 eV initial relative energy.

Fig. 7. The intensity distribution of ND^+ from N^+-HD collisions at 12.3 eV initial relative energy.

Fig. 8. Non-reactive scattering of N^+ by H_2 at 6.87 eV initial relative energy. Note that Q=0 corresponds to elastic scattering, and that Q = -4.5 eV corresponds to collisional dissociation of H_2.

Fig. 9. Non-reactive scattering of N^+ by D_2 at 33.3 eV initial relative energy. The circle labeled impulsive behavior is the locus of possible velocity vectors for N^+ scattered elastically from a single free deuterium atom.

Fig. 10. A partial electronic state correlation diagram for the N^+-H_2 system. At the left, N^+ is assumed to approach H_2 along the perpendicular bisector of the bond. At the right, a collinear approach is assumed. Crossings which are avoided in the more general conformations of C_s symmetry are indicated by dotted lines.

Fig. 11. Product intensity distributions for the reactions of N^+ with H_2 and HD as predicted by the sequential impulse model. The same limiting cardioid applies in each case and at each relative energy. The relative energy for each stability circle is indicated by the values labeled E_r.

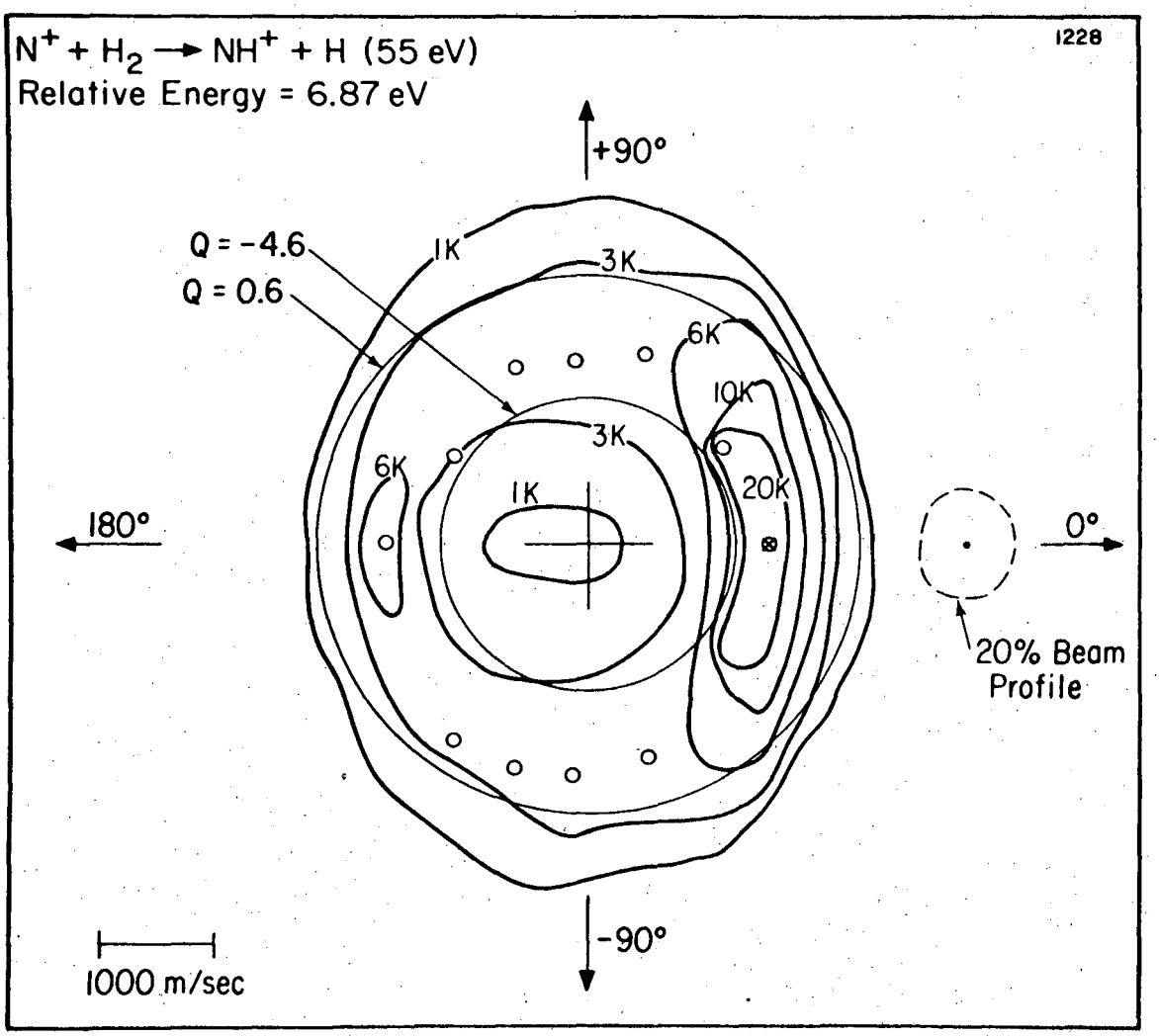
$N^+ + H_2 \rightarrow NH^+ + H$ (55 eV)
Relative Energy = 6.87 eV
1228
+90°
Q = -4.6
Q = 0.6
1K
3K
6K
10K
3K
6K
1K
20K
180°
0°
20% Beam Profile
-90°
1000 m/sec

Fig. 1

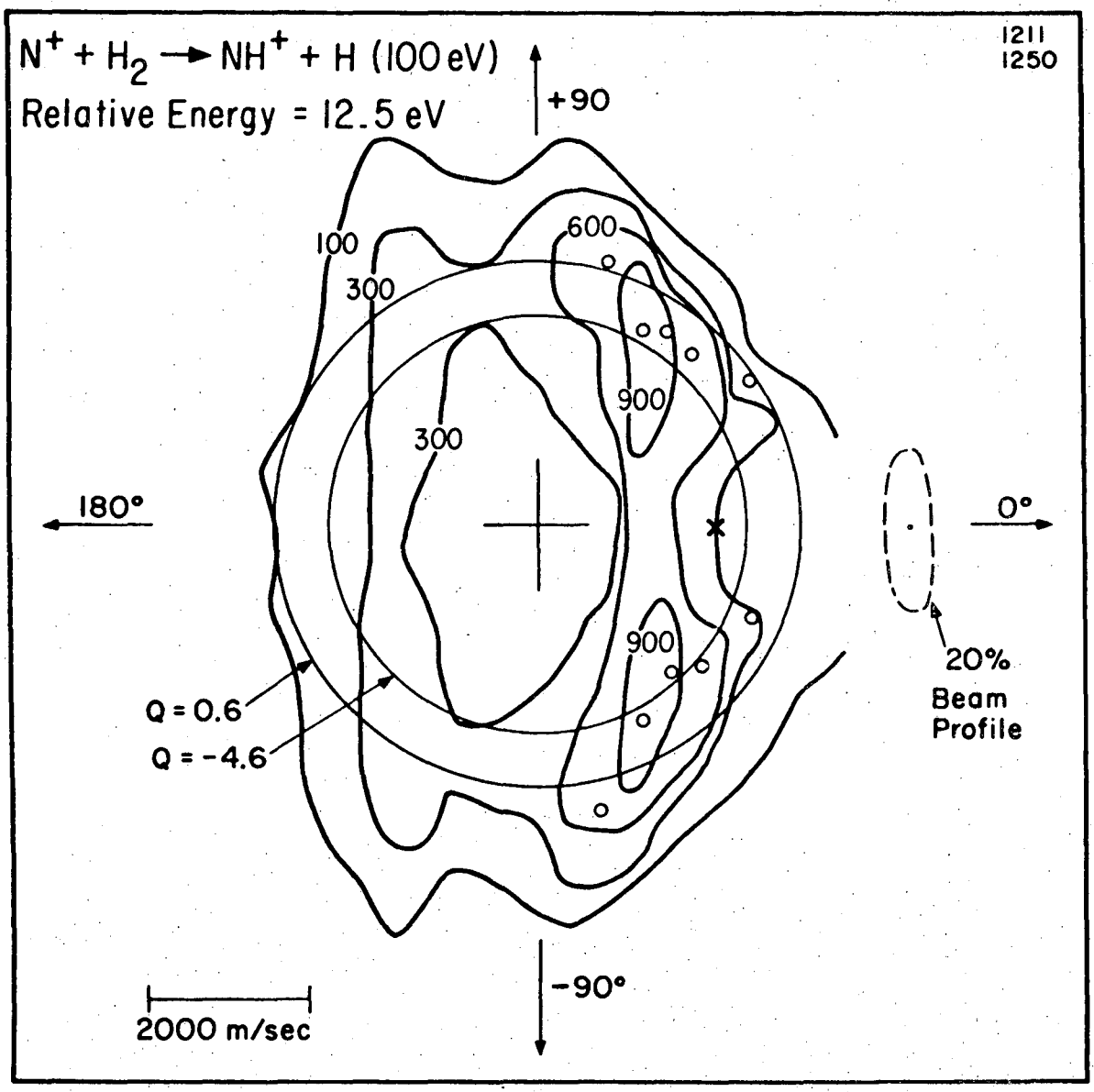

Fig. 2

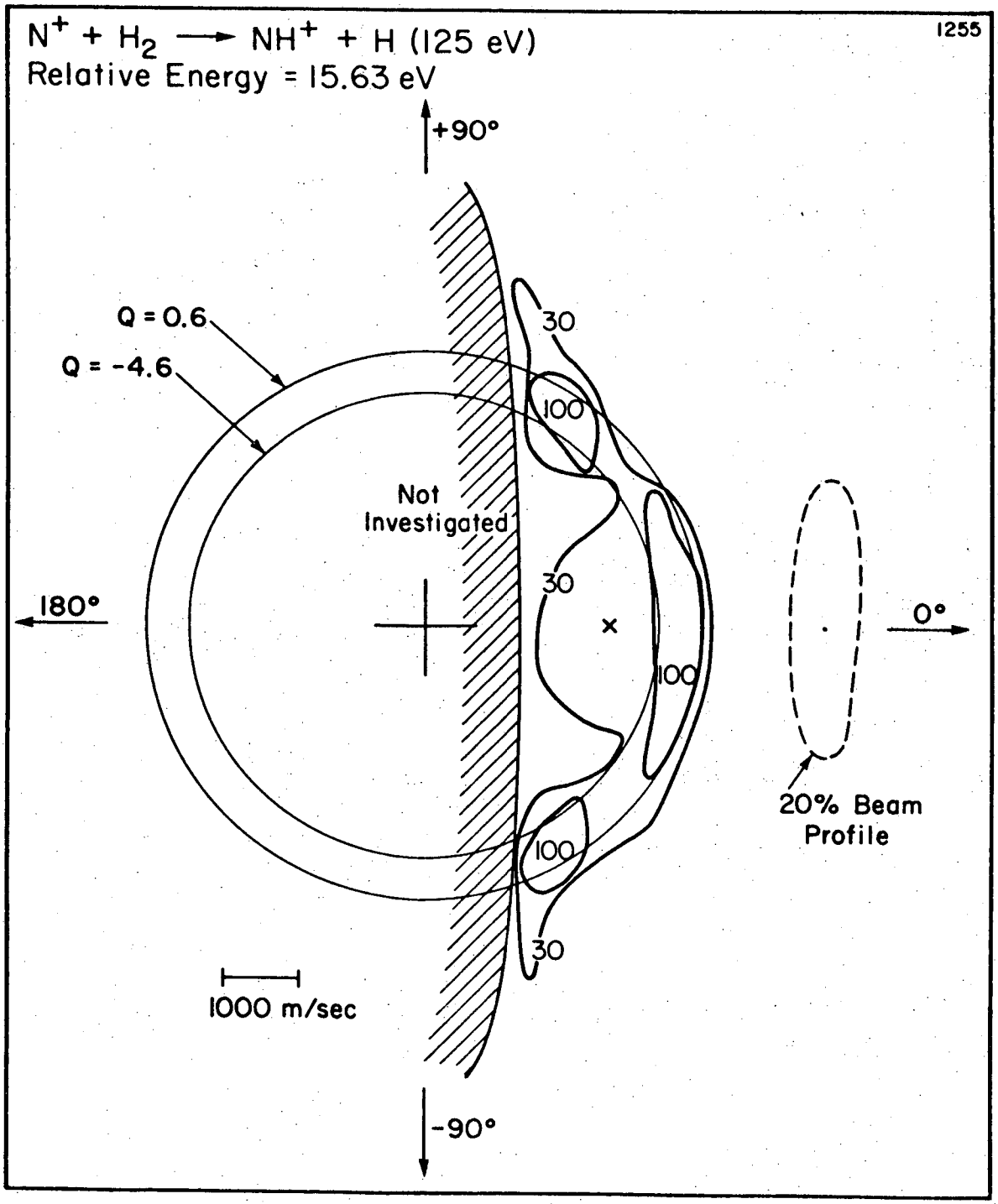
$N^+ + H_2 \longrightarrow NH^+ + H$ (125 eV)
Relative Energy = 15.63 eV
1255
+90°
Q = 0.6
Q = -4.6
30
100
Not Investigated
30
100
100
30
180°
0°
20% Beam Profile
1000 m/sec
-90°

Fig. 3

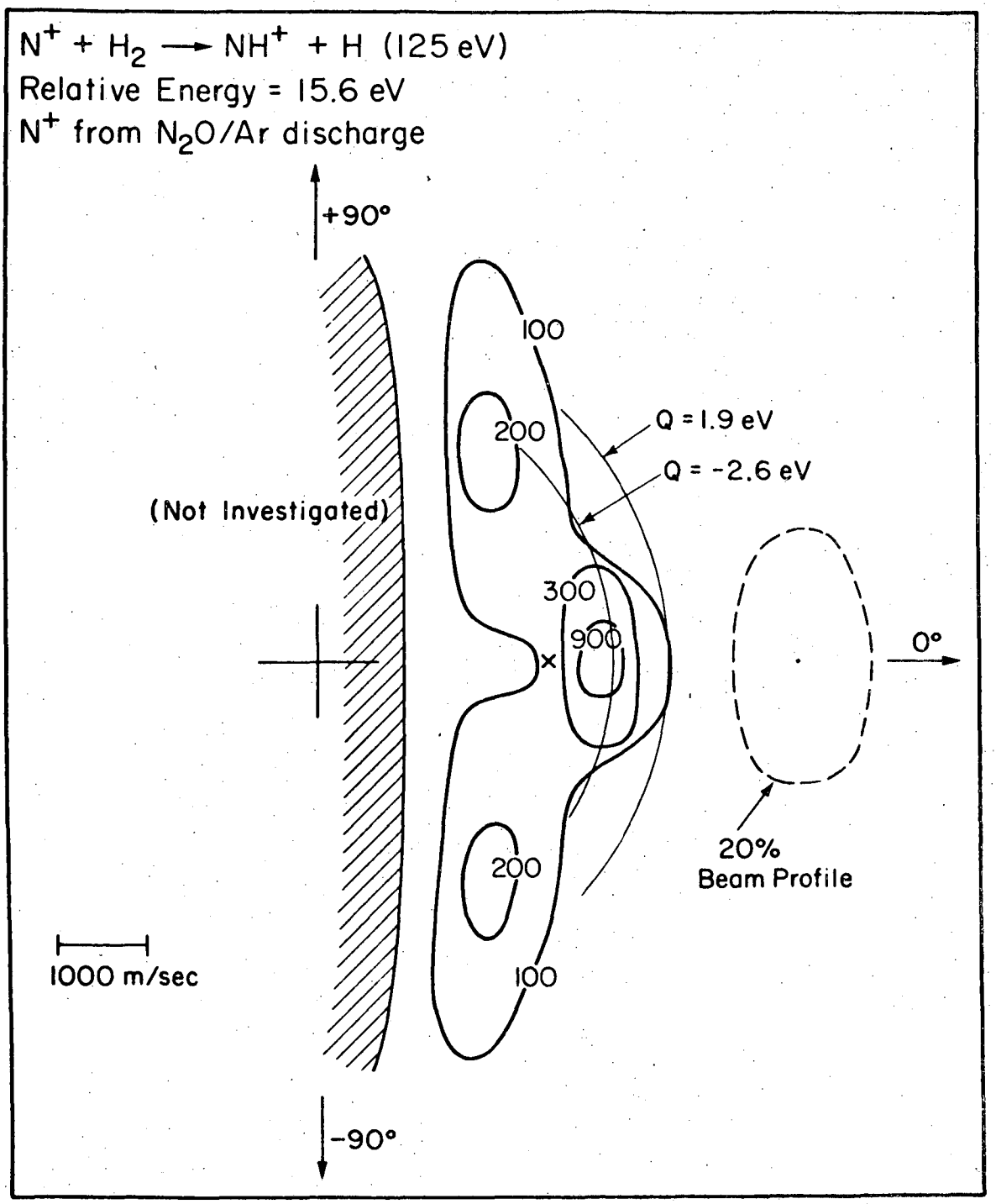

XBL 765-1771a

Fig. 4

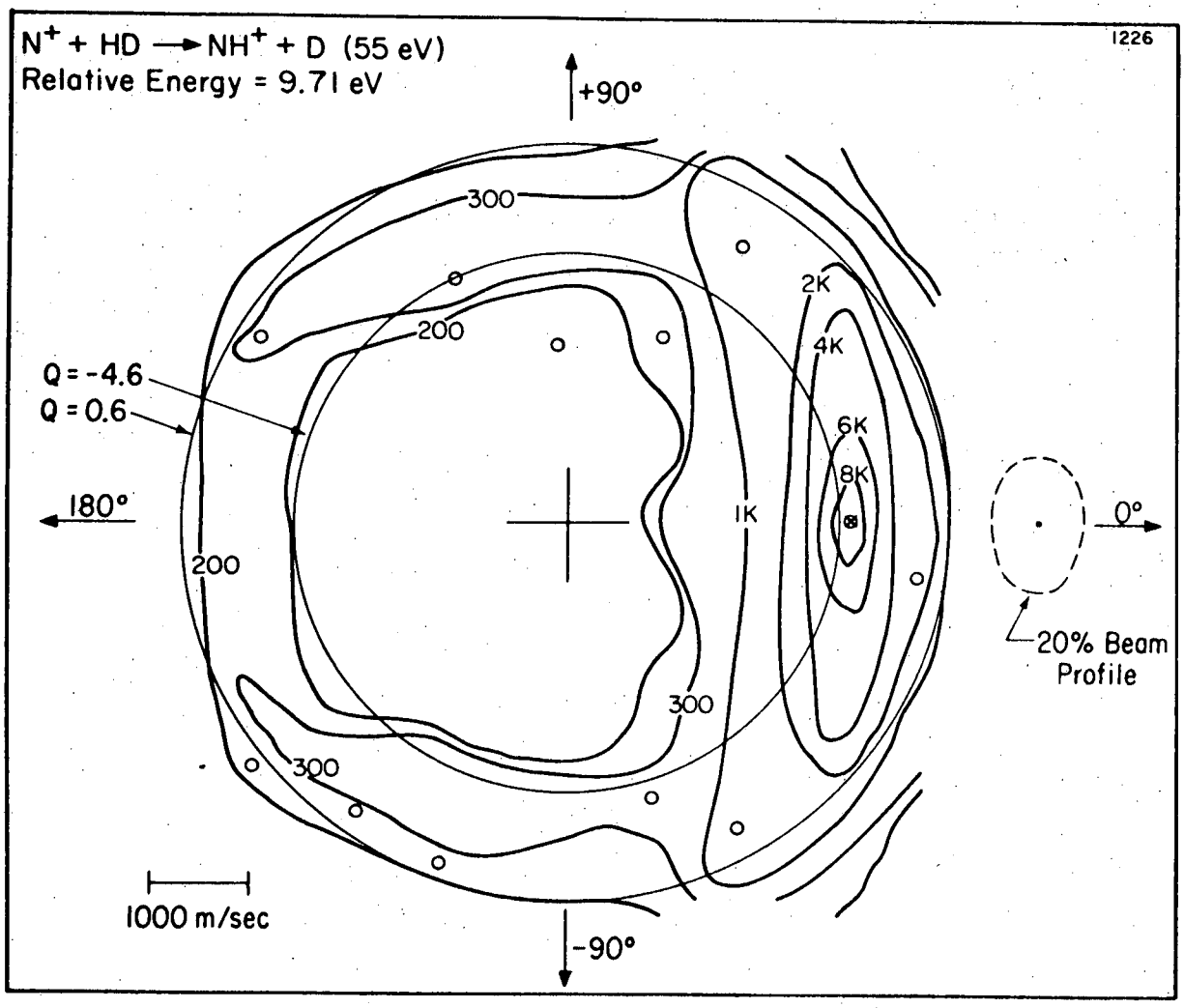
N+ + HD → NH+ + D (55 eV)
Relative Energy = 9.71 eV
1226
+90°
300
200
2K
4K
6K
8K
1K
Q = -4.6
Q = 0.6
180°
0°
200
300
300
20% Beam Profile
1000 m/sec
-90°

Fig. 5

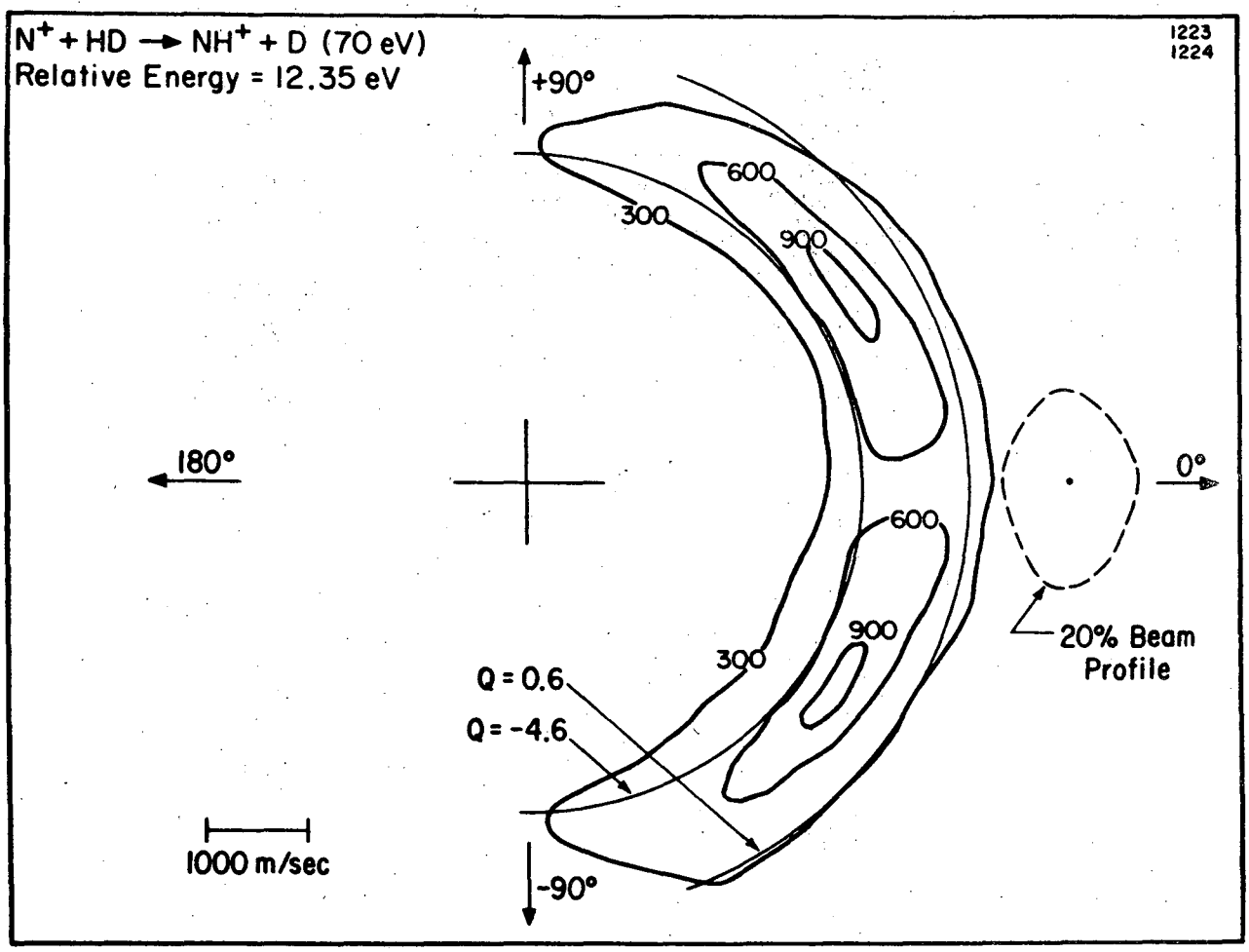

Fig. 6

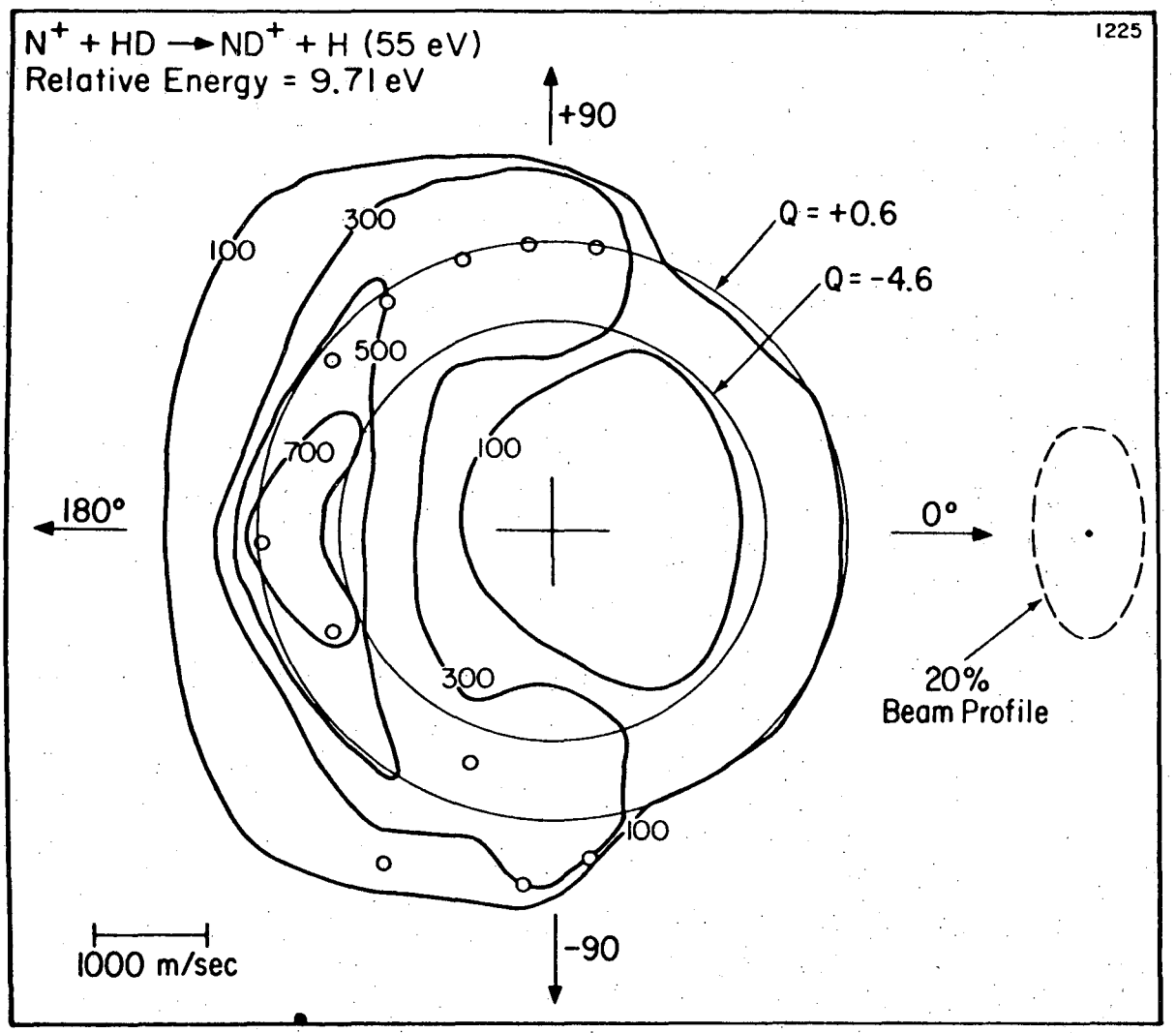
$N^+ + HD \rightarrow ND^+ + H$ (55 eV)
Relative Energy = 9.71 eV
1225
+90
Q = +0.6
Q = -4.6
100
300
500
700
100
180°
0°
300
100
20%
Beam Profile
1000 m/sec
-90

Fig. 7

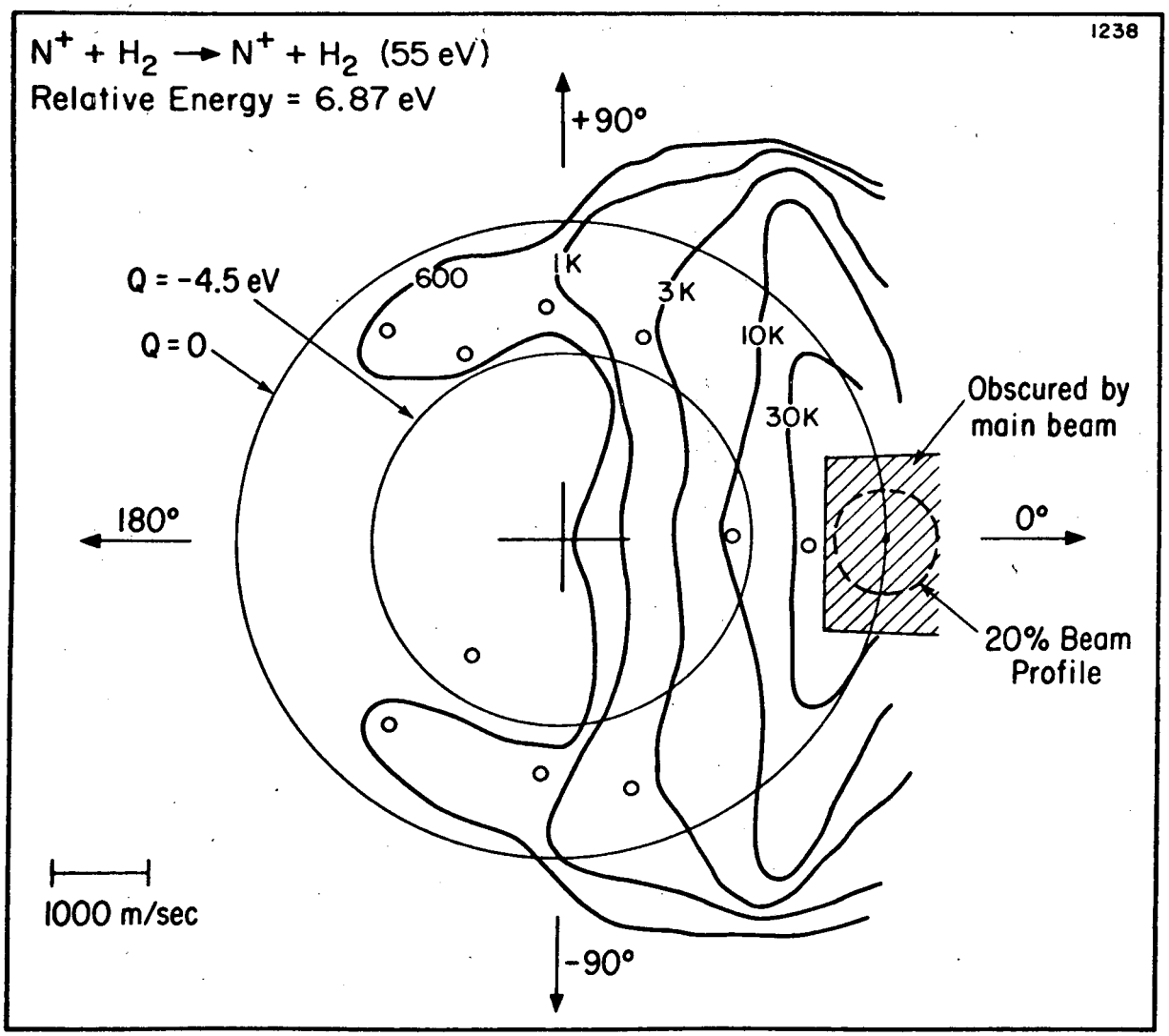

Fig. 8

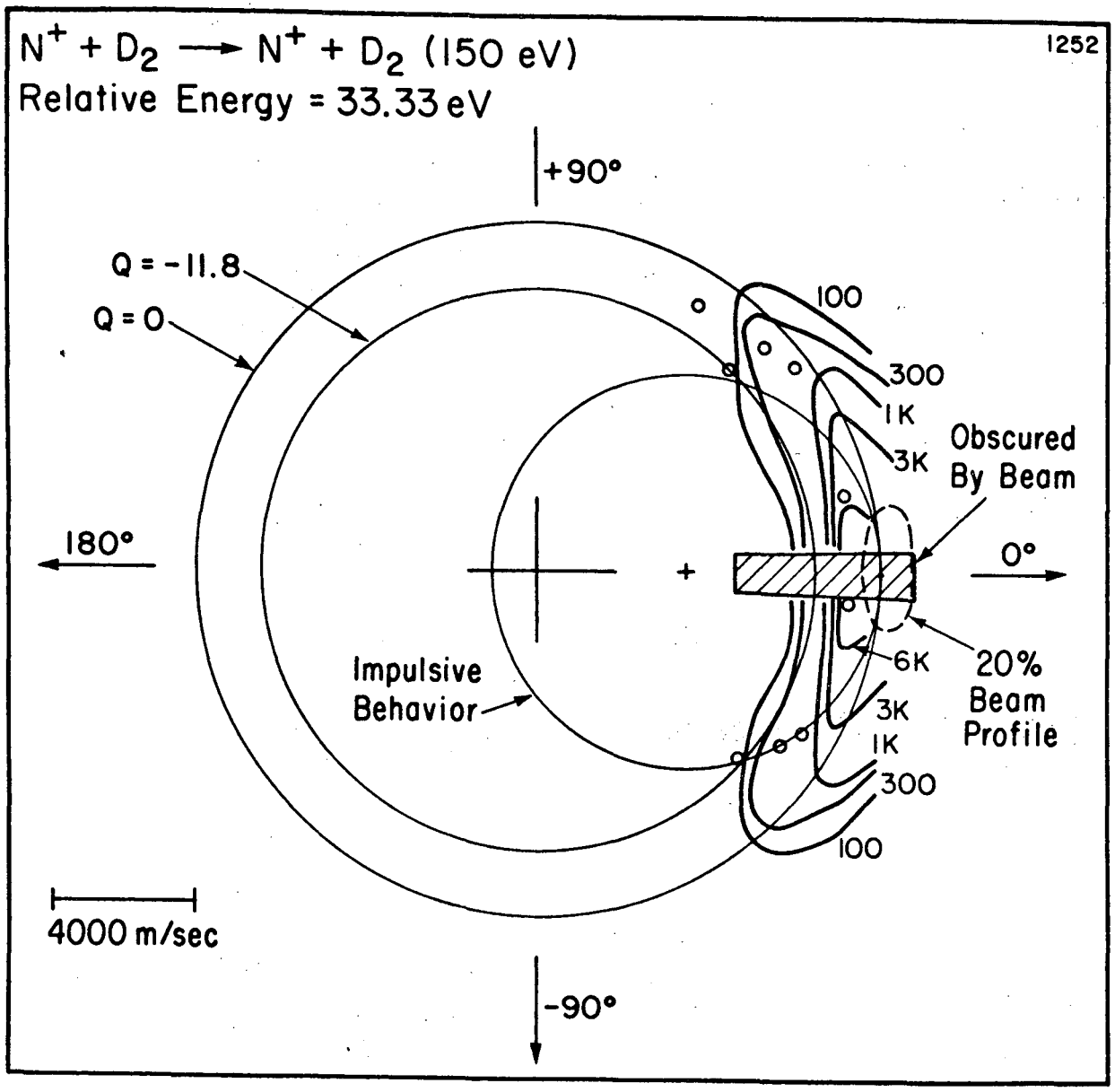
$N^+ + D_2 \longrightarrow N^+ + D_2$ (150 eV)
Relative Energy = 33.33 eV
1252
+90°
Q = -11.8
Q = 0
100
300
1K
3K
Obscured By Beam
180°
0°
6K
20% Beam Profile
Impulsive Behavior
3K
1K
300
100
4000 m/sec
-90°

Fig. 9

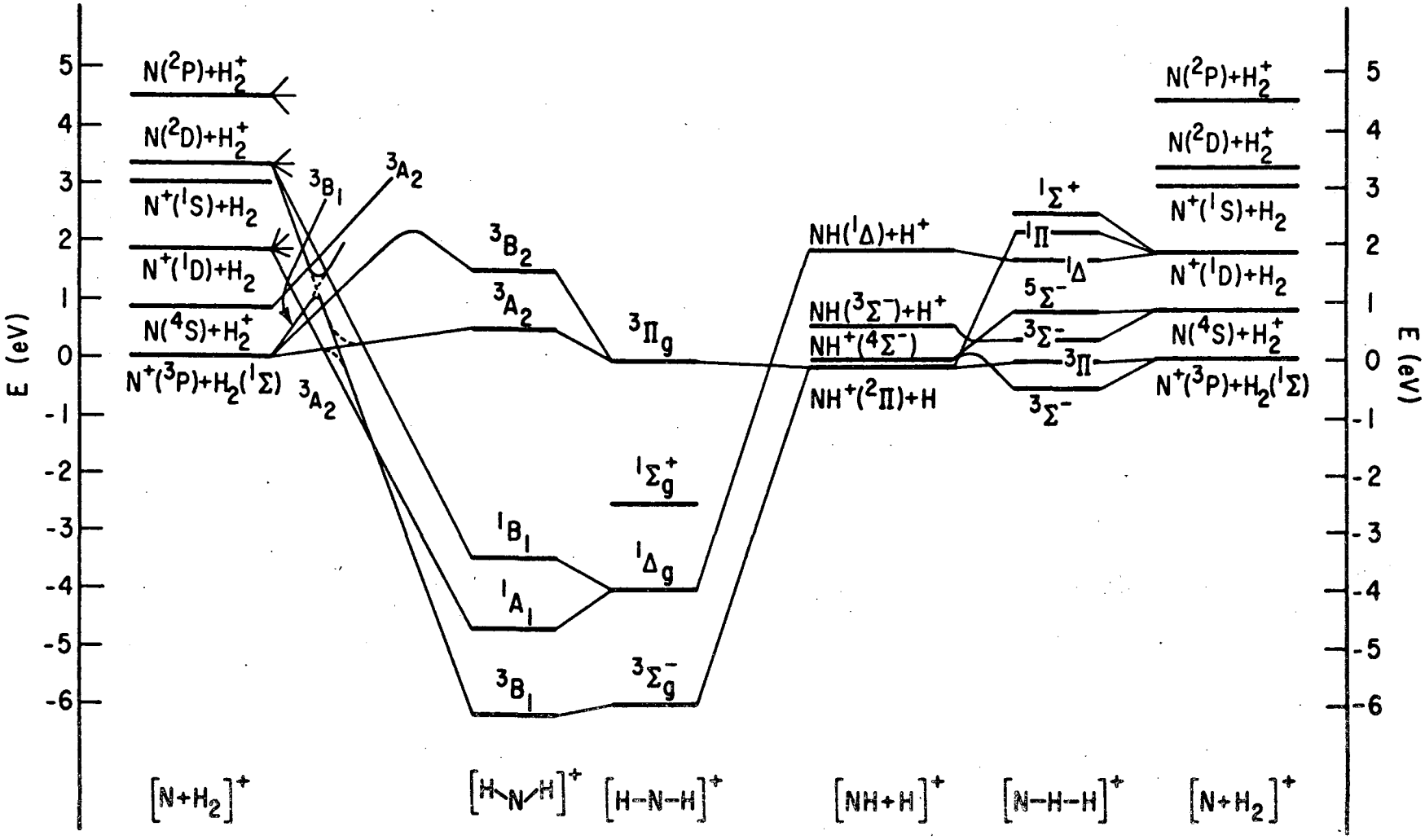
E (eV)
5
4
3
2
1
0
-1
-2
-3
-4
-5
-6
N(2P)+H2+
N(2D)+H2+
N+(1S)+H2
N+(1D)+H2
N(4S)+H2+
N+(3P)+H2(1Σ)
3B1
3A2
3A2
3B2
3A2
3Πg
1Σg+
1B1
1Δg
1A1
3B1
3Σg−
NH(1Δ)+H+
NH(3Σ−)+H+
NH+(4Σ−)
NH+(2Π)+H
1Σ+
1Π
1Δ
5Σ−
3Σ−
3Π
3Σ−
N(2P)+H2+
N(2D)+H2+
N+(1S)+H2
N+(1D)+H2
N(4S)+H2+
N+(3P)+H2(1Σ)
[N+H2]+
[H-N-H]+
[H-N-H]+
[NH+H]+
[N-H-H]+
[N+H2]+

Fig. 10

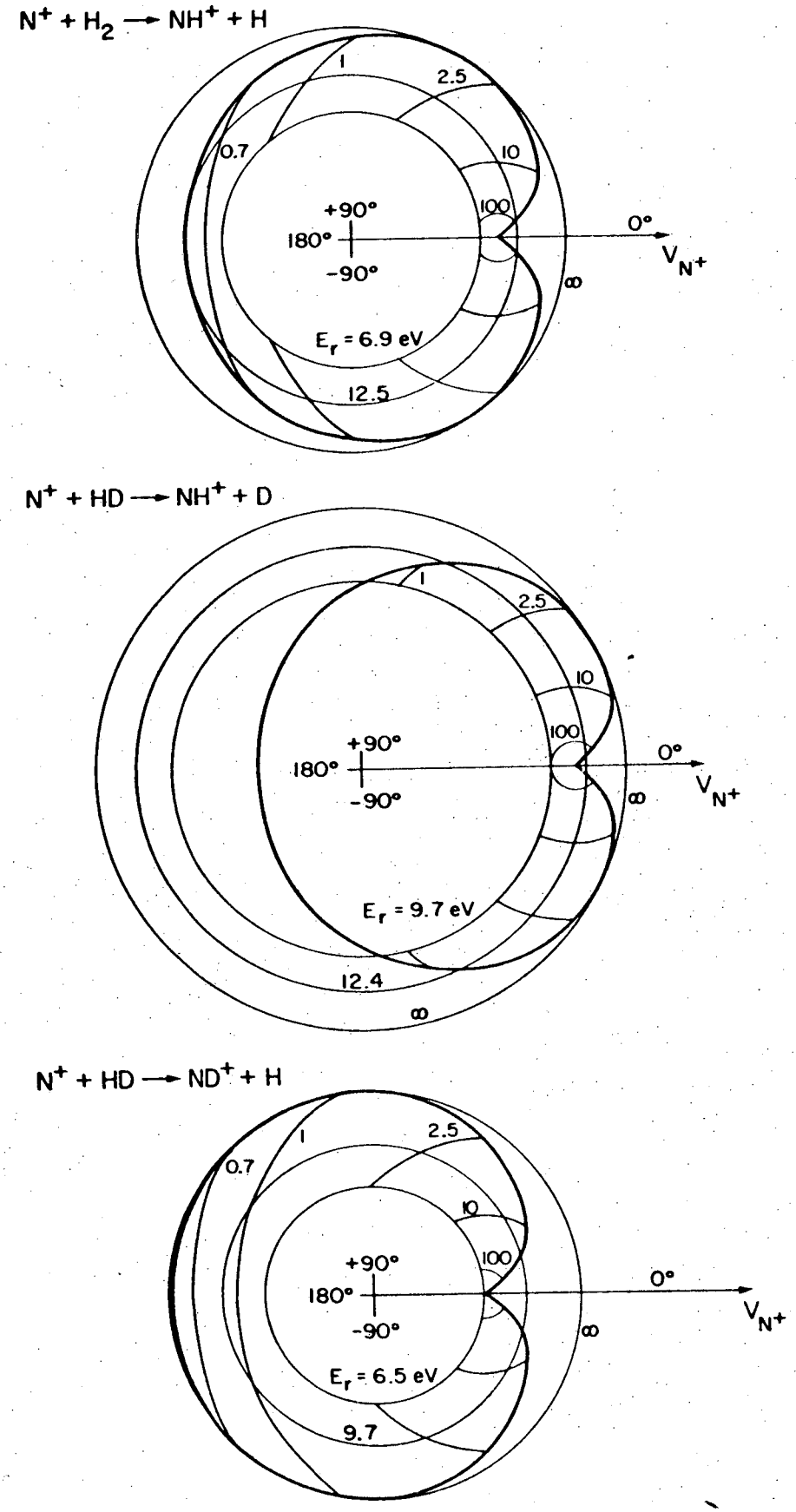
N+ + H2 → NH+ + H
1
2.5
0.7
10
100
+90°
180°
0°
-90°
∞
V_N+
E_r = 6.9 eV
12.5
N+ + HD → NH+ + D
1
2.5
10
100
+90°
180°
0°
-90°
∞
V_N+
E_r = 9.7 eV
12.4
∞
N+ + HD → ND+ + H
1
2.5
0.7
10
100
+90°
180°
0°
-90°
∞
V_N+
E_r = 6.5 eV
9.7

Fig. 11

This report was done with support from the United States Energy Research and Development Administration. Any conclusions or opinions expressed in this report represent solely those of the author(s) and not necessarily those of The Regents of the University of California, the Lawrence Berkeley Laboratory or the United States Energy Research and Development Administration.

TECHNICAL INFORMATION DIVISION
LAWRENCE BERKELEY LABORATORY
UNIVERSITY OF CALIFORNIA
BERKELEY, CALIFORNIA 94720